TESS in the Extended Mission:

A powerful tool for time-domain exoplanet science

Ian Wong[1], Avi Shporer[2]

[1] NASA GSFC (***ian.wong@nasa.gov***); [2] MIT

Abstract

Throughout its two-year Primary Mission, TESS has proven to be an extremely productive tool for studying visible-wavelength exoplanet phase curves (e.g., *Shporer et al. 2019, Wong et al. 2020abc, 2021a*). In July 2020, TESS transitioned to its first Extended Mission, during which it has revisited most of the targets it observed during the Primary Mission and extended its coverage to include part of the near-ecliptic sky. The additional light curves and extended time baseline enable a plethora of scientific investigations into time-domain exoplanet science, including refined full-orbit phase curves, constraints on short- and long-term atmospheric variability, and continuing searches for tidal orbital decay in short-period transiting systems.

Full-orbit phase curves

By examining TESS light curves across the full orbital phase, we have measured the secondary eclipse depth (D_{ecl}) and phase curves for **over 25 transiting systems** (see *Wong et al. 2020b* and *Wong et al. 2021a* for the Primary Mission results). The phase-curve components include the planet's longitudinal atmospheric brightness modulation (A_{atm}), as well as the ellipsoidal distortion (A_{ellip}) and Doppler boosting (A_{Dopp}) of the host star's light.

We primarily used the maximum predicted secondary eclipse depth (assuming geometric albedo of 0.1) as a metric for target selection. Given the increased data volume from the Extended Mission, we expanded our target list for phase-curve study to include fainter stars and systems with smaller predicted signals. We note that the orbital period and number of TESS sectors that a target is observed in also affect the detectability of phase-curve signals.

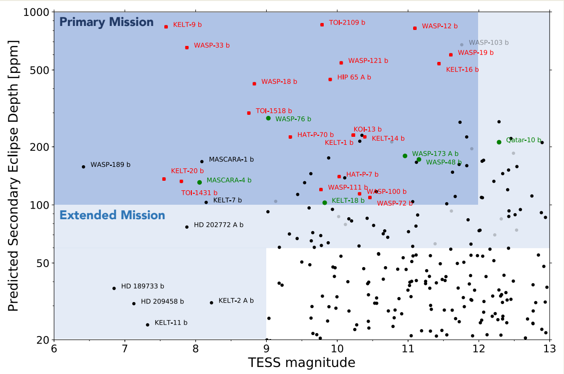

Shaded regions: Target selection areas for our systematic phase-curve analysis

Red: Targets with robust phase-curve detections during the Primary Mission

Green: Targets with newly measured phase curves using data from the Extended Mission

Black: Targets that have no detected phase curve (so far), or targets that have not yet been observed by TESS (e.g., WASP-189 and MASCARA-1)

Gray: Targets in the selection areas that are not observed by TESS during the Primary and Extended Missions (e.g., WASP-103)

Phase-curve highlights

Benchmark systems

For systems with high signal-to-noise phase-curve measurements from the Primary Mission, data from the Extended Mission have yielded significantly improved constraints. For example, in the cases of **WASP-18b and KELT-9b**, the relative precision of the updated D_{ecl} and A_{atm} values rivals that of the highest-quality Kepler phase curves.

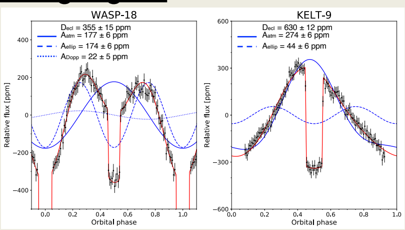

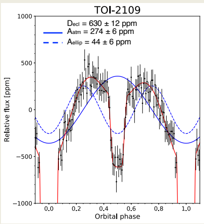

New discoveries

We have uncovered the phase curves of several recently discovered planets detected by TESS. A prominent example is the shortest-period gas giant hitherto known – **TOI-2109b** ($P \sim 0.67$ d, $R_p \sim 1.35\ R_{Jup}$, $M_p \sim 5.02\ M_{Jup}$; *Wong et al. 2021b*) – for which we detected an exquisite phase curve and deep secondary eclipse. From the secondary eclipse depth, we inferred a dayside brightness temperature of **3631 ± 69 K** – the second-hottest yet measured.

Targets from the Extended Mission

The expanded coverage area of TESS in the Extended Mission and additional photometry have produced additional phase-curve detections. The **WASP-76** system, which was not observed during the Primary Mission, was visited by TESS in Sectors 30, 42, and 43. We measured the planet's atmospheric brightness modulation and a robust secondary eclipse, from which we derived the optical geometric albedo (see bottom left).

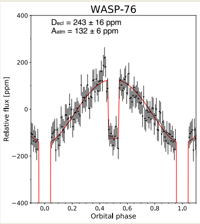

Constraints on atmospheric variability

The repeated TESS observations enable us to place constraints on atmospheric variability across various timescales. For example, **WASP-12** was observed in four sectors, and we measured mutually consistent secondary eclipse depths between individual orbits (black datapoints) and between the sector-wide averages (colored regions). We placed a 2σ upper limit of ~80 ppm (~17%) on dayside brightness variability across month- and year-long timescales. Analogous analyses of other systems (e.g., KOI-13, WASP-18, and WASP-121) have similarly revealed **no evidence for significant atmospheric variability**.

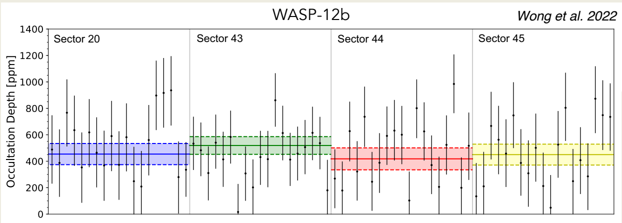

Geometric albedos

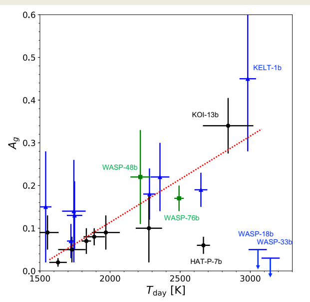

Capitalizing on the synergy between TESS and Spitzer, we used the measured secondary eclipse depths in the optical and infrared to self-consistently calculate the dayside brightness temperatures and optical geometric albedos. **A robust trend between T_{day} and A_g for planets with $1500 < T_{day} < 3000$ K has emerged** (*Wong et al. 2020b, Wong et al. 2021a*).

Improved precision in the measured secondary eclipse depths for Primary Mission targets (blue), as well as Kepler/CoRoT-derived values (**black**) and new additions from the Extended Mission (green), has increased the statistical significance of the correlation to 7.7σ.

Search for tidal orbital decay

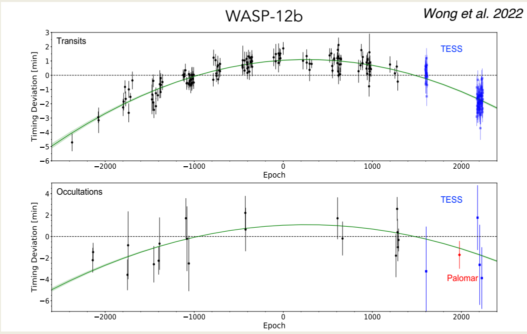

The additional ~2 years of time baseline provided by the TESS Extended Mission will yield improved constraints on long-term transit-timing variations, such as tidal orbital decay.

For **WASP-12b**, we included transit and occultation timings from Sectors 43-45 to obtain an updated period decay rate of **$dP/dt = -29.81 \pm 0.94$ ms/yr**, from which we inferred a host star tidal quality factor of **$Q'_\star = (1.50 \pm 0.11) \times 10^5$**.

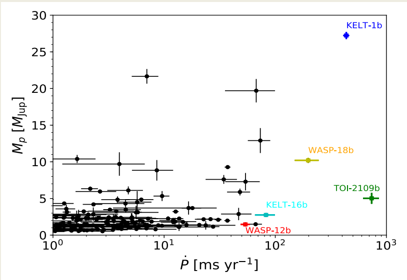

For a given value of the host star's tidal quality factor ($Q'_\star = 10^5$), there are several known transiting objects with higher predicted orbital decay rates. From an analogous transit-timing analysis of the four systems with the highest predicted dP/dt (see plot), we did not find evidence of orbital decay. It follows that the $Q'_\star$ values of the respective host stars must be significantly larger than that of WASP-12 – in the range of $Q'_\star > 4 \times 10^5$.

REFERENCES

Shporer, A., Wong, I., Huang, C.X., et al. 2019, AJ, 157, 178
Wong, I., Benneke, B., Shporer, A., et al. 2020a, AJ, 159, 104
Wong, I., Kitzmann, D., Shporer, A., et al. 2021a, AJ 162, 127
Wong, I., Shporer, A., Daylan, T. et al. 2020b, AJ, 160, 155
Wong, I., Shporer, A., Kitzmann, D., et al. 2020c, AJ, 160, 88
Wong, I., Shporer, A., Vissapragada, S., et al. 2022, AJ, 163, 175
Wong, I., Shporer, A., Zhou, G., et al. 2021b, AJ, 162, 256

DOWNLOAD POSTER HERE